Available online at www.sciencedirect.com
ScienceDirect
Journal of Catalysis 247 (2007) 238–244
JOURNAL OF CATALYSIS
www.elsevier.com/locate/jcat

Reverse effect of doping on stability of principal components of styrene catalyst: $KFeO_2$ and $K_2Fe_{22}O_{34}$

Andrzej Kotarba [a,*], Weronika Rożek [a], Irmina Serafin [a], Zbigniew Sojka [a,b]

[a] *Faculty of Chemistry, Jagiellonian University, Ingardena 3, 30-060 Cracow, Poland*
[b] *Regional Laboratory of Physicochemical Analyses and Structural Research, Ingardena 3, 30-060 Cracow, Poland*

Received 30 November 2006; revised 5 February 2007; accepted 8 February 2007
Available online 12 March 2007

Abstract

The effect of *s* (Mg), *p* (Al), *d* (Cr, Mn), and *f* (Ce) additives (0.25–2 wt%) on the stabilization of constitutional potassium in $KFeO_2$ and $K_2Fe_{22}O_{34}$, the principal phases of styrene catalyst, was investigated by means of a species-resolved (K and K^+) thermal alkali desorption technique. Complementary catalytic screening of the dehydrogenation of ethylbenzene showed that for both ferrites, doping has beneficial effects on selectivity and yield. Spectacular reversal of thermal stability of potassium ferrites on doping was found; whereas doping of $K_2Fe_{22}O_{34}$ resulted in higher stability, as gauged by decreased desorption flux and increased K desorption energy, in the $KFeO_2$ phase, all of the additives caused a dramatic decrease in stability. Thus, phase-specific doping appears to be a critical factor in preventing potassium volatilization from the real catalyst.

Keywords: Styrene catalyst; Potassium ferrite; Thermal desorption; Doping; Potassium stability

1. Introduction

Styrene monomer synthesized by catalytic dehydrogenation of ethylbenzene (EBDH) accounts for >90% of the worldwide production. The endothermic- and equilibrium-limited process is run in industrial units over potassium-promoted iron oxide catalyst in adiabatic conditions, under vacuum at temperatures above 823 K [1]. Promotion with potassium is one of the crucial issues in practical applications, because it increases the activity of the catalyst by an order of magnitude [2]. The commercial catalysts are very active and selective; however, under the process conditions, they deteriorate slowly, and the typical lifetime in the installation is shortened to 1–2 years. Consequently, extensive research has been dedicated to understanding the deterioration mechanism and improving catalyst stability.

In general, two main reasons for the activity decay during the time on stream operation are considered: deposition of excessive carbon and the loss of potassium promoter [3]. Whereas the first factor is reversible, and coke removal is achieved by steam co-feeding, the second factor is irreversible, but can be significantly decreased by solid-state doping with alien metal ions. Classical additives of industrial catalysts include Cr [2,4], Ce [5,6], Mo [7], Al [8], Mg [6,9], and, more recently, Mn [10] and Zn [10,11]. The real iron-oxide catalyst is a multicomponent, multiphase system with the active state assigned to the equilibrium between two ferrites, $KFeO_2 \leftrightarrows K_2Fe_{22}O_{34}$, as discussed in detail by Muhler and Schlögl [8,12,13].

Comprehensive research has been dedicated to potassium loss processes from the real EBDH catalysts [14] and model phases present in the life cycle of the catalyst [15] by the species-resolved thermal alkali desorption (SR–TAD) method. The $K_2Fe_{22}O_{34}$ β-ferrite was explicitly identified as that principally responsible for potassium volatilization from the catalyst [15]. It also has been shown that substitution of Cr^{3+} for octahedral Fe^{3+} ions in $K_2Fe_{22}O_{34}$ structure strongly enhances stabilization of potassium in the temperature range of the industrial process [16]. A similar effect was observed for doping with divalent manganese [17]. The extra-pillars potassium-blocking model was developed to rationalize the stabilization of potassium in the β-ferrite phase. However, up to now there has been

* Corresponding author.
E-mail address: kotarba@chemia.uj.edu.pl (A. Kotarba).

0021-9517/$ – see front matter
doi:10.1016/j.jcat.2007.02.009

no analogous report on the influence of doping on stability of potassium in $KFeO_2$, the second active phase of the catalyst.

The aim of this work is to quantify the effect of chromium, manganese, cerium, aluminum, and magnesium (classic and new promoters reported in literature), on the constitutional potassium volatility from both ferrite phases ($KFeO_2$ and $K_2Fe_{22}O_{34}$) in terms of desorption fluxes and energies.

2. Experimental

The $KFeO_2$ and $K_2Fe_{22}O_{34}$ ferrites were prepared by the reaction of stoichiometric amounts of K_2CO_3 with α-Fe_2O_3 according to procedures described previously [18–20]. The mixtures of finely grounded powders placed in a porcelain crucible were heated with the rate of 7.5 K/min in air up to the final temperatures of 1070 K for $KFeO_2$ and 1470 K for $K_2Fe_{22}O_{34}$. In the latter case, heating was halted at 1170 K, and after cooling to room temperature, the mixture was regrounded for 15 min and reheated at 1470 K for 5 h. For 2 wt% doped samples, the apposite part of α-Fe_2O_3 was replaced by Cr_2O_3, MnO_2, CeO_2, Al_2O_3, and MgO. The doping level of 2 wt% was chosen as the average value of the range applied in industrial practice described in the open and patent literature.

The phase identity of the resultant ferrites was verified after each synthesis by X-ray diffraction using an X'pert Pro Philips powder diffractometer with Cu$K\alpha$ radiation in the Bragg–Brentano geometry. The surface morphology was examined with Philips scanning electron microscope (Model XL 30) at a magnification of $\times$10,000.

The surface composition was studied by XPS (Vacuum Systems Workshop) equipped with an Al anode ($K\alpha = 1486.6$ eV) and hemispherical 150-mm electron analyzer, operated in fixed-analysis transmission mode (FAT) with a pass energy of 22.5 eV.

The catalytic tests for EBDH were carried out in a fixed-bed plug-flow microreactor (4.5 mm i.d., 240 mm long) using 60 mg of a catalyst with a fraction of particle size 0.2–0.3 mm at 550–650 °C ramped in steps of 50 °C. The ethylbenzene (100 μl/h) and water (200 μl/h) were fed to the reaction system with syringe pumps (Cole–Parmer). The reaction products were analyzed by gas chromatography (Varian CP-3800) equipped with a capillary column (Poraplot Q, Chrompack) and a thermal conductivity detector.

The stability of potassium was investigated by the SR-TAD method analogously to the approach applied in [15]. The experiments were carried out in a vacuum apparatus with a background pressure of 10^{-7} mbar. The samples, in the form of wafers of 10-mm diameter with a mass of 100 mg, were heated from room temperature to 700 °C in a stepwise mode at a ramp rate of 5 °C/min. Earlier desorption studies of potassium from styrene catalysts [14,21,22] and related ferrite phases [15,18] demonstrated that the K loss occurs mainly in the form of atoms (in the ground and excited states) and ions. Therefore, to obtain an integral picture of the promoter stability, we followed both K and K^+ desorption fluxes. The desorption flux of potassium atoms (j(K)) was determined by means of a surface ionization detector [23], whereas the flux of K^+ ions ($j(K^+)$) simply by an ion collector. Because the investigated ferrites are efficient electron emitters for quenching the thermal emission of electrons during the measurements, the samples were biased with a positive potential (+10 V for K and +60 V for K^+). This approach effectively eliminates the possibility of reneutralization of K^+ ions by thermal electrons outside the surface. In all of the measurements, the resultant positive current was measured directly with a digital electrometer (Keithley 6512) and averaged over 10 independent data points for each temperature.

3. Results and discussion

3.1. Sample characterization

The diffraction patterns of all of the undoped and doped ferrites revealed that the synthesized samples were essentially monophasic, composed of $K_2Fe_{22}O_{34}$ (JCPDS-ICDD 31-1034) or $KFeO_2$ (JCPDS-ICDD 39-0892). The XRD patterns of all undoped and doped $K_2Fe_{22}O_{34}$ and $KFeO_2$ were indexed within *P6₃/mmc* and *Pbca* space groups, respectively. Examples of the diffraction patterns are shown in Fig. 1. The SEM morphology of the resultant bare and doped $K_2Fe_{22}O_{34}$ showed that the well-developed plate crystallites of hexagonal shape (0.5–2 μm diameter, ~0.2 μm thick) resembled that of a single K^+-β-ferrite with stoichiometric composition [19]. The addition of dopants led to crystallite agglomeration, and the resultant particles exhibited diameters of 5–6 μm for the Mn- and Cr-doped samples and 7–8 μm for the Mg-, Al-, and Ce-doped samples. For the Cr- and Ce-doped β-ferrites, line scan analysis showed partial segregation of these elements on the surface. In the Cr-doped sample, concentration profiles of Cr and K were correlated, suggesting the formation of a new compound (potassium chromate, vide infra). For the Ce-doped β-ferrites, the EDX elemental composition mapping revealed the presence of cerium-containing domains, identified by XRD as CeO_2 using the sample with higher Ce content. $KFeO_2$ showed distinctly different size and morphology, resembling that of the parent α-Fe_2O_3. The small crystallites of about 3–4 μm partly fused to form larger aggregates for all samples (12 ± 3 μm) except the sample doped with Mg, in which the size was somewhat smaller (7 ± 1 μm). Examples of SEM images are available elsewhere [16].

The surface composition of investigated ferrites was studied by XPS. The survey scans indicated that only the constituent elements were present within the surface layer. For $K_2Fe_{22}O_{34}$- and $KFeO_2$-doped samples, the observed binding energies were essentially independent of the dopant nature, indicating that all of the constituents exhibited a unique oxidation state consistent with the stoichiometry of both ferrites. The characteristic binding energies were in line with previous, more detailed studies [24] with the particular values of Fe $2p_{3/2}$ (710.2–710.4 eV), K $2p_{3/2}$ (294.4–294.5 eV), and O 1s (529.4–529.5 eV) for $K_2Fe_{22}O_{34}$, whereas for $KFeO_2$, they slightly shifted to Fe $2p_{3/2}$ (709.7–710.0 eV), K $2p_{3/2}$ (292.2–292.4 eV), and O 1s (530.4–530.8 eV). The diagnostic binding energies for the Mn (641.0 eV), Al (73.6 eV), Mg (1303.2 eV), and Cr (576.8 and 579.3) for doped $K_2Fe_{22}O_{34}$ and Mn (642.4 eV), Al (72.5 eV),

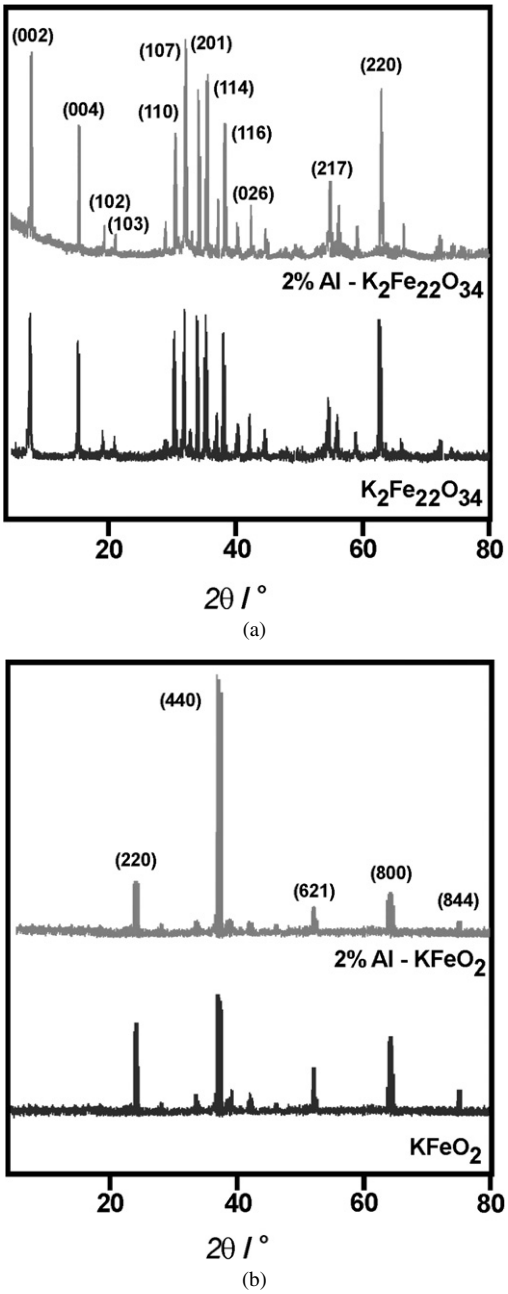

Fig. 1. The diffraction patterns of undoped and 2 wt% Al-doped potassium ferrites $K_2Fe_{22}O_{34}$ (a) and $KFeO_2$ (b).

Mg (1303.8 eV), and Cr (578.9) for $KFeO_2$ revealed that the Mn, Al, and Mg dopants existed in a single state in both ferrites. In the case of chromium, two oxidation states, Cr^{3+} and Cr^{6+}, were found in the $K_2Fe_{22}O_{34}$, and only one oxidation states (Cr^{3+}) was found in the 2% Cr-$KFeO_2$. The appearance of two kinds of chromium in $K_2Fe_{22}O_{34}$ can be associated with the partial surface segregation of this dopant in the form of chromate [16]. In the case of cerium, a weak, poorly structured band (six overlapping peaks $3d_{5/2}$, $3d_{3/2}$, and four satellites [25]) was observed at 883–917 eV. This finding is in line with the SEM and XRD observations of intensive CeO_2 agglomeration causing the decreased amount of Ce exposed to the surface detectable by XPS.

The samples were next subjected to the catalytic screening in EBDH. In most cases, a positive effect of doping on catalytic performance was found. At 650 °C, the styrene yield varied from 58.7% for bare $K_2Fe_{22}O_{34}$ to 76.0, 73.0, 71.2, 59.5, and 44.3% for Cr-, Mg-, Al-, Ce-, and Mn-doped $K_2Fe_{22}O_{34}$, respectively. For $KFeO_2$, the yield of styrene changed from 51.3 to 70.4, 57.5, 54.3, 52.4, and 49.7% for the Cr-, Mg-, Mn-, Ce-, and Al-doped samples, respectively. In addition, the two phases, $K_2Fe_{22}O_{34}$ and $KFeO_2$, were brought intentionally into intimate contact in the model composite catalyst prepared by a two-step procedure: (1) ceramic synthesis of separate $K_2Fe_{22}O_{34}$ and $KFeO_2$ and (2) sintering at 800 °C [26]. Compared with the separate phases, a significant increase in the conversion of ethylbenzene to styrene (to 62.3%) was observed. This nicely corroborates previous reports on the importance of $K_2Fe_{22}O_{34} \leftrightarrows KFeO_2$ equilibrium to catalytic reactivity. Thus, the studies performed for the thin K–Fe–O films deposited on Ru(0001) and Pt(111) substrates under ultrahigh vacuum conditions [13,24] are confirmed by the more realistic results obtained using bulk materials.

Therefore, from the sample characterization it may be inferred that on doping at the level of 2 wt%, the basic structural and morphological characteristics of both ferrites were successfully preserved. This means that the principal location of potassium remained unchanged on introduction of the dopants. At the same time, the dopants exhibited a pronounced promotional effect on catalytic performance, thereby justifying their application in practice.

3.2. Potassium thermal stability

The K and K^+ desorption fluxes from undoped and doped β-ferrites are shown in Figs. 2a and 2b, respectively. For all of the samples, $j(\mathrm{K}) > j(\mathrm{K}^+)$, meaning that the main channel of potassium loss from the catalyst is due to atoms. The loss of potassium then can be considered a volatilization process. According to the Saha–Langmuir equation [27], the domination of the atomic flux in the desorption process indicates that the work function of the samples must be lower than the ionization potential of potassium (4.3 eV). Indeed, the work functions of the $K_2Fe_{22}O_{34}$ and $KFeO_2$ ferrites determined in parallel experiments of electron thermionic emission were found to be 2.2 and 2.5 eV, respectively.

For the undoped β-ferrite, the onset of appreciable K desorption was observed at about 400 °C, whereas for substituted ones, it rose to above 550 °C. The monotonous exponential changes of the signal with temperature indicate that in each case, the potassium left the surface effectively trough a single potential barrier. Therefore, the corresponding desorption energies were determined from the linear part of the Arrhenius-type plots [$\ln(j(\mathrm{K}^+))$ or $\ln(j(\mathrm{K}))$ vs $1/T$] for atoms and ions. The values are collected in Table 1. The desorption energy for potassium atoms changed from 0.83 eV ($K_2Fe_{22}O_{34}$) to 2.35–4.05 eV on doping. This difference in desorption energies is reflected in a dramatic quenching of the potassium volatilization gauged by the K-flux intensity (Fig. 2). For ionic desorption, the energies ranged from 2.33 eV for $K_2Fe_{22}O_{34}$ to 2.05–3.47 eV

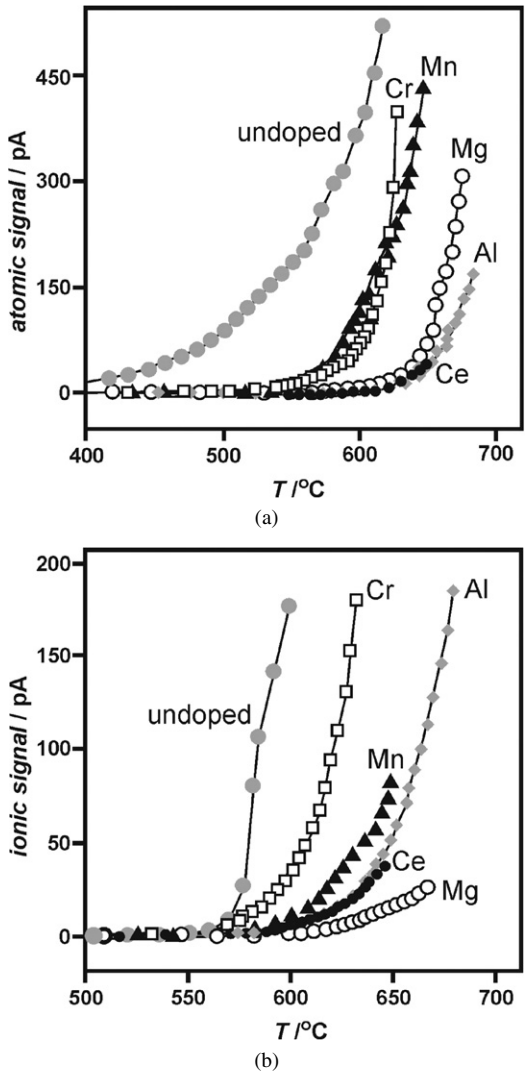

Fig. 2. The changes of atomic (a) and ionic (b) desorption fluxes from $K_2Fe_{22}O_{34}$ phase upon 2 wt% of doping.

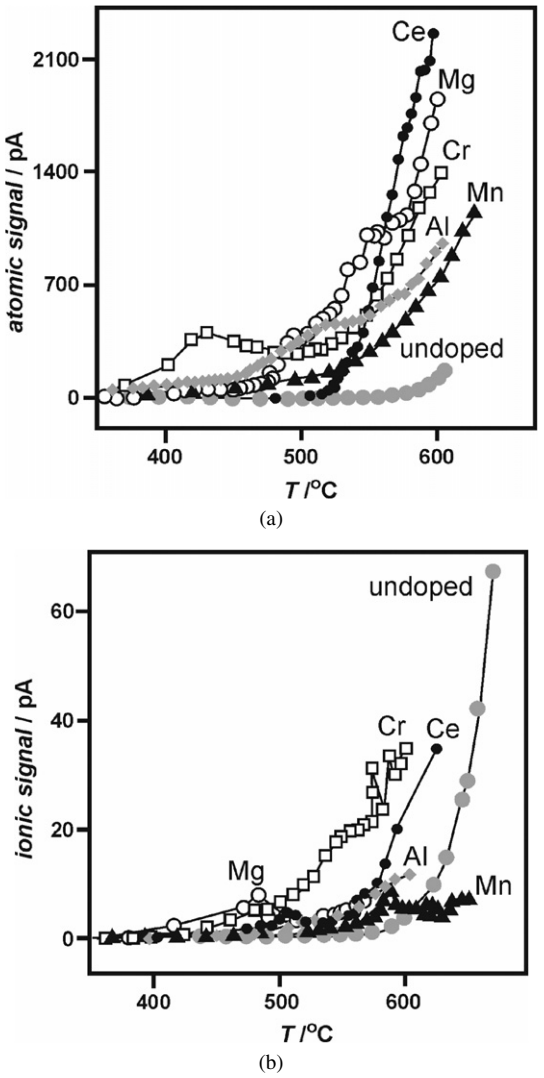

Fig. 3. The changes of atomic (a) and ionic (b) desorption fluxes from $KFeO_2$ phase upon 2 wt% of doping.

Table 1
Activation energies for K and K^+ desorption from undoped and doped potassium ferrites

Sample	E_d(K) (eV)	$E_d(K^+)$ (eV)	Reference
$K_2Fe_{22}O_{34}$	0.83 ± 0.01	2.33 ± 0.03	[13]
2% Cr-$K_2Fe_{22}O_{34}$	2.23 ± 0.01	3.47 ± 0.01	This work
2% Mn-$K_2Fe_{22}O_{34}$	2.35 ± 0.03	3.39 ± 0.01	[15]
2% Mg-$K_2Fe_{22}O_{34}$	2.71 ± 0.03	2.05 ± 0.03	This work
2% Al-$K_2Fe_{22}O_{34}$	3.54 ± 0.02	3.56 ± 0.02	This work
2% Ce-$K_2Fe_{22}O_{34}$	4.05 ± 0.02	2.86 ± 0.01	This work
$KFeO_2$	2.84 ± 0.06	2.95 ± 0.01	[13]
2% Mn-$KFeO_2$	1.12 ± 0.03	1.51 ± 0.01	[9]
2% Cr-$KFeO_2$	1.04 ± 0.01	0.90 ± 0.02	This work
2% Ce-$KFeO_2$	0.98 ± 0.01	2.01 ± 0.01	This work
2% Mg-$KFeO_2$	0.96 ± 0.01	0.60 ± 0.04	This work
2% Al-$KFeO_2$	0.68 ± 0.03	1.12 ± 0.02	This work

Note. The energies were calculated for the correlation coefficient higher that 0.98 and the errors correspond to 95% confidence limit.

for doped $K_2Fe_{22}O_{34}$. The lower desorption energies for atoms and the resulting domination of the atomic fluxes are characteristic of oxide surfaces in the measured temperature range [28].

Fig. 3 shows atomic and ionic flux intensity profiles for the fresh and doped $KFeO_2$ ferrite as a function of temperature. In contrast to $K_2Fe_{22}O_{34}$, in this case a dramatic increase in atomic desorption flux occurred on doping above 500 °C. This is reflected in the decreased desorption energies for atoms (2.84 eV for undoped to 0.68–1.12 eV for doped) and ions (2.95 for undoped to 0.60–2.01 eV for doped). The low-temperature maxima on some curves represent the volatilization of loosely bound surface potassium. However, such surface-segregated potassium, being only a minute fraction of the main K-flux, cannot be relevant for the practical loss of the potassium from the catalyst.

The energy diagram ($E_d(K^+)$ vs E_d(K)) [15,17] for $K_2Fe_{22}O_{34}$ and $KFeO_2$ was used to evaluate the effect of additives on the stability of potassium (Fig. 4). A totally different picture emerged from the comparison of both figures. Whereas for the $K_2Fe_{22}O_{34}$ phase, doping led to stability enhancement, for $KFeO_2$, it had a clearly negative effect. It is noteworthy that the destabilization effect in $KFeO_2$ was more pronounced than the

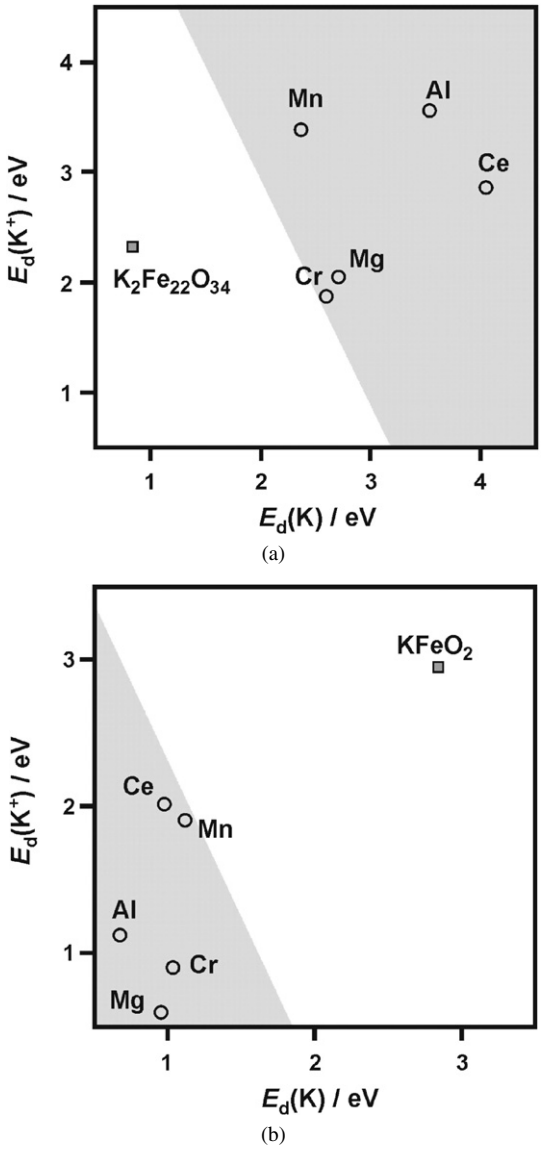

Fig. 4. Stability diagram: desorption energies of potassium ions and atoms plotted against each other, showing the increase of stability of $K_2Fe_{22}O_{34}$ (a) and decrease in the case of $KFeO_2$ (b) upon introduction of 2 wt% of various additives.

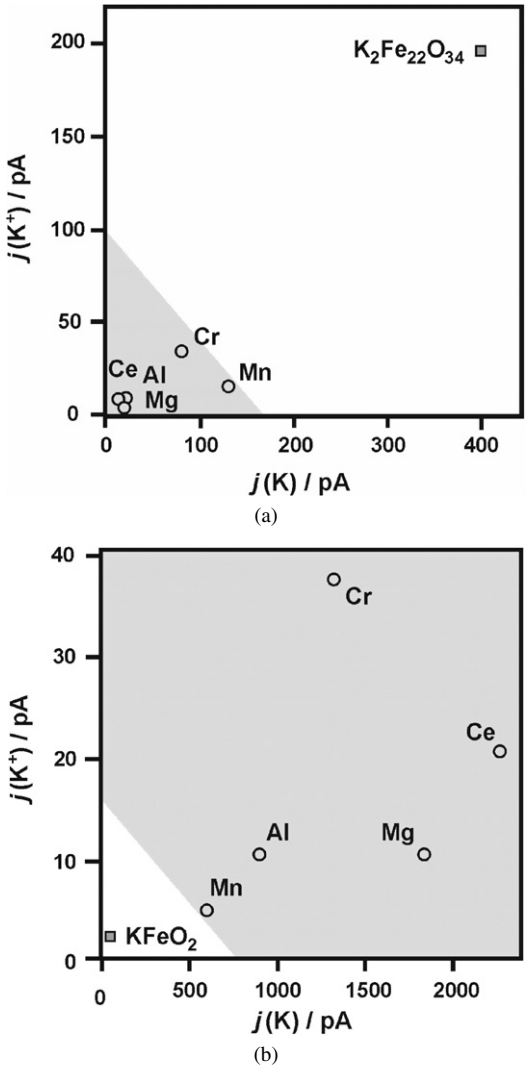

Fig. 5. Stability diagram: desorption fluxes of potassium ions and atoms plotted against each other, showing the increase of stability of $K_2Fe_{22}O_{34}$ (a) and decrease in the case of $KFeO_2$ (b) upon introduction of 2 wt% of various additives.

stabilization effect in $KFe_{22}O_{34}$ (as shown by the shaded areas in Fig. 4).

Because desorption of K from iron oxide materials can involve several steps (e.g., diffusion from the bulk, surface diffusion between sites of different desorption energies, electronic switching to highly excited states, formation of clusters), the pre-exponential factor for the alkali desorption process can vary widely [29]. Depending on conditions and catalyst composition, various steps can appear as the rate-limiting process. In particular, if the excited states are formed during thermal desorption, then the measured pre-exponential coefficients change within the wide range of 10^4–10^{23} s^{-1} [29]. This means that the desorption fluxes, being the actual measure of potassium loss, may not follow the desorption energetics directly. Fig. 5 presents the stability diagram in terms of desorbing fluxes, again showing the reverse effect on constitutional potassium stability in both investigated ferrites. For $K_2Fe_{22}O_{34}$, the quenching of potassium loss is seen, whereas for $KFeO_2$ the loss process is enhanced dramatically.

3.3. Implication for catalyst preparation

The main role of additives in industrial K–Fe–O catalysts is to stabilize the active state of the catalyst under the process conditions by preventing potassium volatilization. In the wet environment of industrial processes, potassium removal from the catalyst and migration though the catalytic bed is expected to occur in the form of KOH. This concept, originally advanced by Mross [30] and revisited by Schlögl et al. [31], can be easily reconciled with our results. In the case of the structural modifiers, potassium diffusion from the bulk of the β-ferrite is inhibited, resulting in the observed spectacular decrease in K desorption flux (Figs. 2 and 5), accompanied by an increase in the desorption barrier (Fig. 4). In the presence of ∼0.1 mbar of water vapor, subsequent in situ transformation

of the nascent potassium into highly surface spread KOH can occur quite readily. This supposition is well supported by the fact that the surface of the spent catalyst is usually decorated with KOH [3]. Thus, inhibition of the constitutional potassium diffusion from the bulk toward the catalyst surface effected by doping prevents undesired onsite formation of KOH. However, in several types of experiments with molecular beam and mass spectrometric methods, the potassium loss process via KOH in a commercial iron oxide catalyst was not observed [32,33]. In our experiments, when H_2O or KOH were intentionally placed on the surface of $KFeO_2$ or $K_2Fe_{22}O_{34}$, a small QMS signal of KOH desorbing flux at 650 °C was detected; nevertheless, this desorption pathway was always less than one-third of the dominating atomic flux. A more detailed study of the effect of water vapor on potassium volatilization is currently in progress.

Two main mechanisms along which the additives can stabilize potassium in the ferrite phases can be considered. The first involves steric blocking of the interlayer diffusion pathway by formation of extra-pillars in the conducting plane. The second involves an increase in the work function of the catalytic surface, leading to decreased domination of the potassium loss atomic flux.

The first mechanism is well illustrated in the case of Cr dopant [16]. Joint Mössbauer spectroscopy and XPS indicated that Cr^{3+} ions, due to their high octahedral crystal field stabilization energy, substitute for Fe^{3+} ions. The latter, in turn, are displaced to the interlayer space, forming new extra-pillars Fe_t–O–Fe_t, on filing tetrahedral sites. Because potassium transport to the surface is controlled by the diffusion through the conducting plane (001), the steric hindrance generated by new pillars effectively blocks the diffusion pathway. This model can be extended onto the other divalent and trivalent ions, such as Mg^{2+}, Mn^{2+}, and Al^{3+}. These may either displace the octahedral iron into tetrahedral sites to form the blocking pillars or occupy the tetrahedral sites in the interlayer space to create the pillars directly [16].

The second possible mechanism relies on the modification of surface electronic properties. Following the Saha–Langmuir equation [27], the statistical probability ratio of ionic to atomic potassium desorption fluxes is exponentially dependent on the work function value,

$$\frac{j(\mathrm{K}^+)}{j(\mathrm{K})} = \frac{1}{2}\exp\left[\frac{-e(V_\mathrm{K} - \Phi)}{k_\mathrm{B}T}\right],$$

where V_K, Φ, k_B, and T denote ionization potential of desorbing atom (for potassium 4.3 eV), work function of the surface, Boltzmann constant, and temperature, respectively. Thus, the atomic flux can be attenuated by an increase in the work function. Because desorption of K^+ leads to charge separation, this channel of potassium loss apparently is less important at the macroscopic scale. Unfortunately, strict quantitative treatment of the fluxes following the Saha–Langmuir equation is impossible, because the desorption of electronically excited, easily ionized potassium atoms observed experimentally for ferrites [14,18,21] obscures the ratio of atomic flux to ionic flux. Therefore, the experimental data can be treated only semiquantitatively for any responsible deductions. Nevertheless, the general trends can be inferred from Fig. 5 quite reliably. In $KFeO_2$, the observed changes in the $j(K^+)/j(K)$ ratio on doping are more pronounced, indicating that the electronic factor plays a more significant role than it does in $K_2Fe_{22}O_{34}$. Thus, the stabilization effect due to the addition of dopant can result from both the structural and electronic modification of the active phases of the iron oxide catalyst. In addition, our investigations indicate quite clearly that for practical purposes, phase-selective doping of $K_2Fe_{22}O_{34}$ is essential to prevent excessive potassium loss while maintaining catalytic activity.

4. Conclusion

Dramatic changes in stability of the $K_2Fe_{22}O_{34}$ and $KFeO_2$ active phases of the styrene catalyst on doping with Cr, Mn, Ce, Al, and Mg were revealed by thermal desorption of potassium atoms and ions. The accommodation of additives in $K_2Fe_{22}O_{34}$ phase significantly increased the K and K^+ desorption energies and extinguished the dominating desorption atomic flux by an order of magnitude. The reverse effect was observed in the case of $KFeO_2$, where the additives led to pronounced thermal destabilization of potassium. Thus, doping of the $K_2Fe_{22}O_{34}$ phase exclusively is required to prepare a robust catalyst with suitable activity and enhanced thermal stability of constitutional potassium under the operating conditions used in this study.

Acknowledgment

This work was sponsored by the National Committee for Scientific Research of the Polish Ministry of Science and Higher Education (research project 3T09B14026).

References

[1] D. Resasco, in: I.T. Horvath (Ed.), Encyclopedia of Catalysis, vol. 3, Wiley, Hoboken, 2003, p. 76.
[2] K. Kochloefl, in: G. Ertl, H. Knözinger, J. Weitkamp (Eds.), Handbook of Heterogeneous Catalysis, vol. 5, VCH, Weinheim, 1997, p. 2151.
[3] G.R. Meima, P.G. Menon, Appl. Catal. A Gen. 212 (2001) 239.
[4] N. Dulamita, A. Maicaneanu, D.C. Sayle, M. Stanca, R. Cracium, M. Olea, C. Afloroaei, A. Fodor, Appl. Catal. A Gen. 287 (2005) 9.
[5] A. Trovarelli, C. De Leitenburg, M. Loaro, G. Dolcetti, Catal. Today 50 (1999) 353.
[6] T. Hirano, Appl. Catal. 26 (1986) 65;
T. Hirano, Appl. Catal. 28 (1986) 119.
[7] F. Cavani, F. Trifiro, Appl. Catal. A Gen. 133 (1995) 219.
[8] M. Muhler, J. Schütze, M. Wesemann, T. Rayment, A. Dent, R. Schlögl, G. Ertl, J. Catal. 126 (1990) 339.
[9] T. Hirano, Bull. Chem. Soc. Jpn. 59 (1986) 2672.
[10] A. Miyakoshi, A. Ueno, M. Ichikawa, Appl. Catal. A Gen. 216 (2001) 137;
A. Miyakoshi, A. Ueno, M. Ichikawa, Appl. Catal. A Gen. 219 (2001) 249.
[11] H.E.L. Bomfim, A. Conceição Oliveira, M. do Carmo Rangel, React. Kinet. Catal. Lett. 80 (2003) 359.
[12] M. Muhler, R. Schlögl, G. Ertl, J. Catal. 138 (1992) 413.
[13] G. Ketteler, G. Ranke, R. Schlögl, J. Catal. 212 (2002) 104.
[14] L. Holmlid, P.G. Menon, Appl. Catal. 212 (2001) 247.
[15] A. Kotarba, I. Kruk, Z. Sojka, J. Catal. 211 (2002) 265.

[16] I. Serafin, A. Kotarba, M. Grzywa, Z. Sojka, H. Bińczycka, P. Kuśtrowski, J. Catal. 239 (2006) 137.
[17] A. Kotarba, I. Kruk, Z. Sojka, J. Catal. 221 (2004) 650.
[18] A. Kotarba, A. Barański, S. Hodorowicz, J. Sokołowski, A. Szytuła, L. Holmlid, Catal. Lett. 67 (2000) 129.
[19] S. Ito, H. Kurosawa, K. Akashi, Y. Michiue, M. Watanabe, Solid State Ionics 86 (1996) 745.
[20] S. Ito, M. Washio, I. Makino, N. Koura, K. Akashi, Solid State Ionics 86 (1996) 1005.
[21] L. Holmlid, K. Engvall, C. Aman, P.G. Menon, Stud. Surf. Sci. Catal. 75 (1992) 795.
[22] K. Engvall, L. Holmlid, Appl. Surf. Sci. 55 (1992) 303.
[23] K. Engvall, L. Holmlid, A. Kotarba, J.B.C. Pettersson, P.G. Menon, P. Skaugset, Appl. Catal. A Gen. 134 (1996) 239.
[24] Y. Joseph, G. Ketteler, C. Kuhrs, W. Ranke, W. Weiss, R. Schlögl, Phys. Chem. Chem. Phys. 3 (2001) 4141.
[25] G. Praline, B.E. Koel, R.L. Hance, H.I. Lee, J.M. White, J. Electron Spectrosc. Relat. Phenom. 21 (1980) 17.
[26] W. Rożek, A. Kotarba, Z. Sojka, in preparation.
[27] G.A. Samorjai, in: Introduction to Surface Chemistry and Catalysis, Wiley, New York, 1994, p. 376.
[28] T.E. Madey, B.V. Yakshinsky, V.N. Ageev, R.E. Johnson, J. Geophys. Res. 103 (1998) 5873.
[29] L. Holmlid, J. Phys. Chem. A 102 (1998) 10636.
[30] W.D. Mross, Catal. Rev. Sci. Eng. 24 (1983) 591.
[31] O. Shekhah, W. Ranke, R. Schlögl, J. Catal. 255 (2004) 56.
[32] J. Lundin, K. Engvall, L. Holmlid, P.G. Menon, Catal. Lett. 6 (1990) 85.
[33] K. Engvall, L. Holmlid, P.G. Menon, Appl. Catal. 77 (1991) 235.